ELSEVIER

Journal of Hazardous Materials B137 (2006) 138–143

Journal of Hazardous Materials

www.elsevier.com/locate/jhazmat

Sintered glass ceramic composites from vitrified municipal solid waste bottom ashes

Mirko Aloisi, Alexander Karamanov *, Giuliana Taglieri, Fabiola Ferrante, Mario Pelino *

Department of Chemistry, Chemical Engineering and Materials, University of L'Aquila, Monteluco di Roio 67040, Italy

Received 13 December 2003; received in revised form 7 October 2005; accepted 14 December 2005
Available online 28 March 2006

Abstract

A glass ceramic composite was obtained by sinter-crystallisation of vitrified municipal solid waste bottom ashes with the addition of various percentages of alumina waste. The sintering was investigated by differential dilatometry and the crystallisation of the glass particles by differential thermal analysis. The crystalline phases produced by the thermal treatment were identified by X-ray diffraction analysis. The sintering process was found to be affected by the alumina addition and inhibited by the beginning of the crystal-phase precipitation. Scanning electron microscopy was performed on the fractured sintered samples to observe the effect of the sintering. Young's modulus and the mechanical strength of the sintered glass ceramic and composites were determined at different heating rates. The application of high heating rate and the addition of alumina powder improved the mechanical properties. Compared to the sintered glass ceramic without additives, the bending strength and the Young's modulus obtained at 20 °C/min, increased by about 20% and 30%, respectively.
© 2006 Elsevier B.V. All rights reserved.

Keywords: Glass ceramic; Composite material; Sintering; Crystallisation; Industrial waste

1. Introduction

In 2004, 44 incinerators (31 with electric energy production and 10 with thermal energy recovery) were operating in Italy resulting in 2.6 million tonnes of waste being disposed [1]. Depending on the chemical composition and the results of the leaching tests, the solid residues of the thermal treatment (i.e. bottom and fly ashes) are usually classified as special or hazardous wastes. Presently they are disposed in landfill sites [2].

Vitrification is a known technology used to improve the chemical stability prior to disposal. It has been applied to nuclear waste [3–5] as well as to several hazardous industrial residues [6–9]. By properly selecting the glass composition and thermal treatment, the re-utilisation of the glass or glass ceramic as raw material for different industrial applications can be obtained. In this regard, several studies have been carried out in recent years on the crystallisation behaviour of the parent glass obtained from MSW ashes, on the structure and properties of bulk glass ceramics and on the possibility of obtaining sintered glass ceramic and composites from powdered MSW glasses [10–18].

Sinter-crystallisation is a technology based on a combined sintering of the glass particles and crystal-phase formation induced by the thermal treatment [19–22]. Glass powders are used to produce glass ceramics (GC) and composites [23,24] by means of a fast thermal treatment. Improved mechanical properties, high chemical durability and complex shapes can be obtained.

In previous studies, the sintering behaviour of a glass obtained by Vercelli Municipal Solid Waste Incinerator was presented [17,18]. In the present study, the sinter-crystallisation behaviour of glass ceramics composites obtained using the same glass with the addition of different amounts alumina waste is investigated. The sintering and crystallisation were studied by dilatometric measurements and by differential thermal analysis (DTA) at different heating rates, respectively. The crystalline phases formed were evaluated by X-ray diffraction (XRD) and the structure of the obtained sintered glass ceramics was observed by scanning electron microscopy (SEM). The mechanical properties of the glass ceramics and composites obtained at different heating rates were compared.

* Corresponding authors. Tel.: +39 0862 434233; fax: +39 0862 434233.
E-mail addresses: karama@ing.univaq.it (A. Karamanov), pelino@ing.univaq.it (M. Pelino).

0304-3894/$ – see front matter © 2006 Elsevier B.V. All rights reserved.
doi:10.1016/j.jhazmat.2005.12.056

Table 1
Chemical composition of the BA, GC0 and AW

	BA	GC0	AW
SiO_2	40.9	41.1	1.4
TiO_2	1.2	2.9	–
Al_2O_3	13.6	14.0	97.6
Fe_2O_3	5.7	4.1	0.2
CaO	12.2	13.9	0.5
MgO	3.1	4.6	0.3
Na_2O	10.9	10.3	–
K_2O	1.8	3.2	–
Other	Balance	Balance	Balance

2. Experimental

The bottom ash (BA) vitrification was performed in alumina crucibles at 1400 °C for 1 h in air in a chamber furnace. The resulting dark brown glass, labelled GC0, was quenched. The BA, GC0 and alumina waste (AW) compositions were determined by XRF (Spectro Xepos). The results are shown in Table 1.

The glass was broken, milled and sieved to obtain different granulometric fractions. In the present study, the fraction passing 75 μm is used. The GC0 glass ceramics were prepared through the sinter-crystallisation of the parent glass powder while the composites, labelled GC10, GC20 and GC30, were obtained with the addition of 10, 20 and 30 wt.% AW (<75 μm).

The initial samples were obtained by mixing the powder glass and the alumina waste powders with 10% PVA (polyvinyl alcohol) solution and by uniaxially pressing at 100 MPa at room temperature. Samples (9 mm × 4 mm × 3 mm and 50 mm × 4 mm × 3 mm) were shaped to study the sintering and to measure the mechanical properties of the obtained glass ceramics.

The crystallisation behaviour of GC0 and GC20 was investigated by differential thermal analysis (DTA-Netzsch STA 409) at 10 °C/min heating rate in the 20–1250 °C range. The sintering of composites was investigated by dilatometer (Dilatometer Netzsch 402ED) measuring the shrinkage of the samples in the 700–1000 °C temperature range at different heating rates. The morphology of the fractured sintered samples was observed by scanning electron microscopy (SEM Philips XL30CP). The crystalline phases induced by the thermal treatment were identified by XRD analysis (Philips-PW 1830, Cu Kα) and the formed total amount of crystalline phase was evaluated by comparing the area of amorphous halo in the parent glass and GC0 [19]. The open porosity, P, was estimated through the relation: $P\,(\%) = 100\,(\rho_{sk} - \rho_{app})/\rho_{sk}$, where ρ_{app} is the apparent density, measured by Dry Flow pycnometer (GeoPyc 1360), and ρ_{sk} is the skeleton density, measured by Helium displacement Pycnometer (AccyPyc 1330).

The mechanical strength was determined by the three-points bending test with a 40-mm outer span and a crosshead speed of 0.1 mm/min (SINTEC D/10) by using series of five samples. The Young's modulus of the sintered glass ceramics was determined by means of the non-destructive resonance frequency technique (Grindosonic).

3. Results and discussion

In the previous studies, carried out with GC0 composition glass ceramic [17,18], two overlapping crystallisation peaks were present in the DTA traces corresponding to 440 and 430 kJ/mol activation energies of crystallization. Based on XRD and SEM, crystallisation started as a surface pyroxene formation, followed by anorthite and gehlenite in the bulk.

Fig. 1 shows the DTA plot of GC0 and GC20 and demonstrates that both samples have similar crystallisation behavior. The glass transformation temperatures (T_g) are relatively high and occur at about 669 and 665 °C for GC0 and GC20, respectively. The crystallisation exo-peaks, T_p, are detected at 859 and 920 °C, and 863 and 925 °C for GC0 and GC20 respectively. The melting endo-effects occurs in range of 1160–1200 °C for both samples. The temperature interval between T_p and T_g is shorter than the temperature interval between the liquidus temperatures, T_l, and T_p, indicating a relatively high crystallisation trend [25,26]. The T_l was detected at about 1160 °C as the onset of the curve while the maximum of the endo-effect was revealed at about 1200 °C. Thus, the alumina addition does not sensibly influence the crystallisation process of the glass matrix.

This result was also confirmed by the XRD spectra of the glass ceramic and composites, shown in Fig. 2. The XRD of GC0 show that the crystalline phases formed are pyroxene – $Fe_xMg_yCa_{(1-x-y)}SiO_3$, anorthite – $CaAl_2Si_2O_8$ and gehlenite – $Ca_2Al_2SiO_7$. The total percentage of the crystalline phase formed after 1 h heat treatment at 1000 °C was 67 ± 3%, where the associated error is an overall estimation of the uncertainties related to the evaluation of the areas in the XRD spectrum [19]. In GC10, GC20 and GC30, the same phases (pyroxene, anorthite and gehlenite) with the same relative ratio were identified. The corundum peak intensity is consistent with the increasing amount of AW.

Since crystallisation and sintering occurred simultaneously, the densification in GC0 was inhibited and a residual porosity remained in the glass ceramic. The sintering rate was shown to

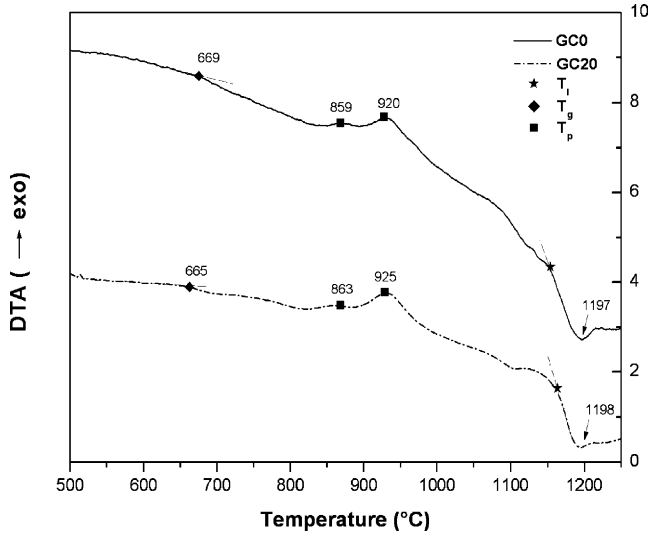

Fig. 1. DTA traces of GC20, GC0 powder (<75 μm) at 10 °C/min heating rate.

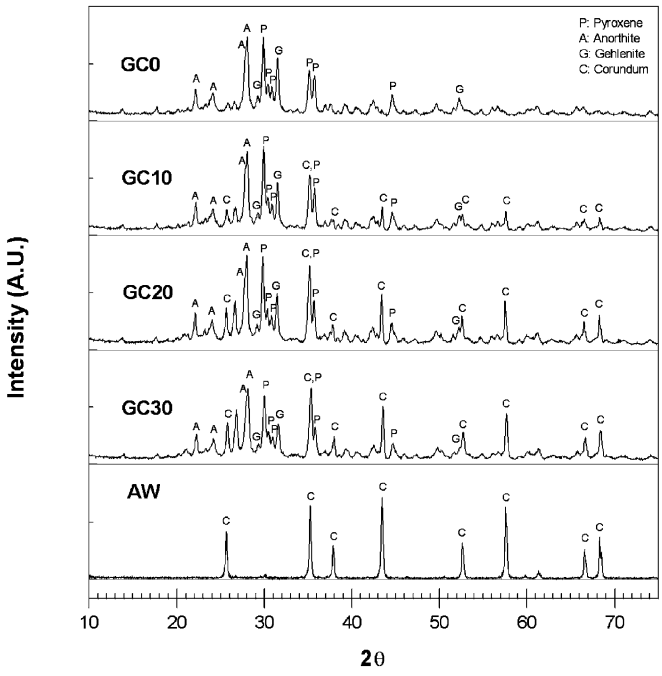

Fig. 2. XRD patterns of GC0, AW and composites heated up to 1000 °C.

decrease due to the beginning of the pyroxene formation and the densification stopped in the temperature range 800–850 °C after a formation of about 10% crystal phase [18].

The dilatometric results of the composites obtained at 10 °C/min are reported in Fig. 3a. The GC10 sample reached a maximum shrinkage of 13% whereas, for GC20 and GC30 shrinkage of 12% and 9.5% was obtained, respectively.

In Fig. 3b, the sintering rate of the composite is plotted. In agreement with the Scherer theory on composite densification, at the beginning of sintering, the rate decreases by increasing the amount of AW [27,28]. The maximum densification rate occurs at almost the same temperature, 802–806 °C. After the maximum, the curves of all composites practically coincide due

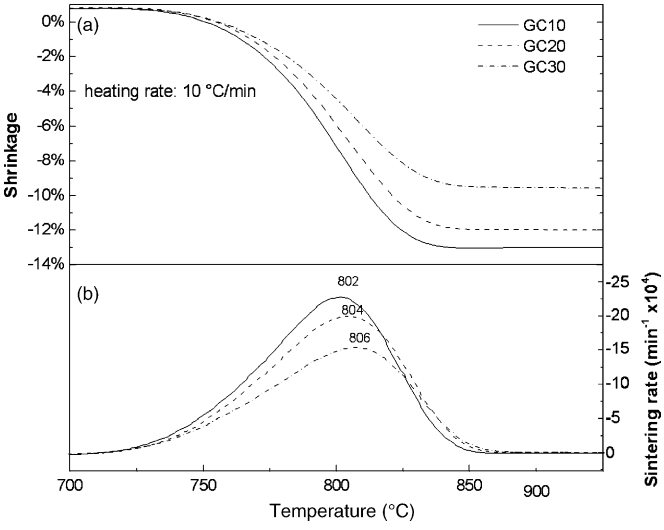

Fig. 3. Dilatometric shrinkage and sintering rate of the composites during densification at 10 °C/min up to 1000 °C.

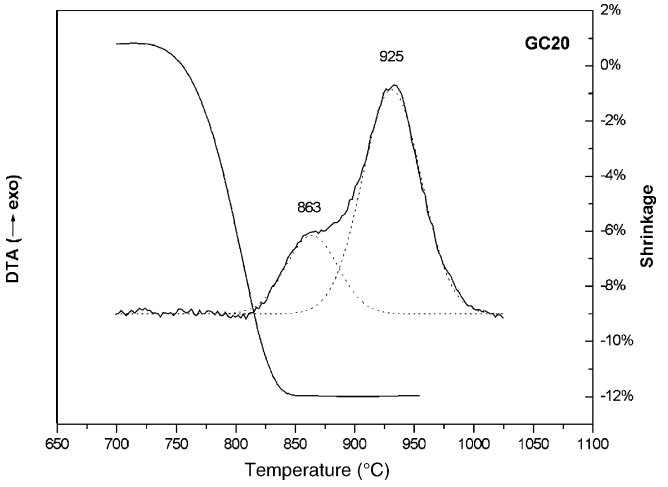

Fig. 4. DTA trace and dilatometric shrinkage of GC20.

to the beginning of the phase formation and the rate is reduced to zero at 850 °C (i.e. identical behaviour as GC0 glass ceramic [18]). The results show a similar densification degree for GC10 and GC20, while for GC30, it is considerable lower. For this reason, the sinter-crystallisation behaviour of the composites was investigated in detail for GC20 composition.

Fig. 4 compares the GC20 sintering curve and the corresponding DTA trace. The exo-effect in the DTA trace is shown by the overlapping of two peaks. The first peak is due to the beginning of precipitation of pyroxene, whereas the second peak is due to the other crystalline phases [17]. The sintering plot shows that the densification is inhibited by the beginning of the crystalline-phase formation in the glass matrix. The same behaviour was observed in GC0 and other sintered glass ceramics [18,22,29].

Fig. 5 presents the GC20 dilatometric curves obtained at 5, 10 and 20 °C/min. The densification improves at a high heating rate: the shrinkage reaches 13% at 20 °C/min, 12% at 10 °C/min and only 10% at 5 °C/min. The residual porosity values for the

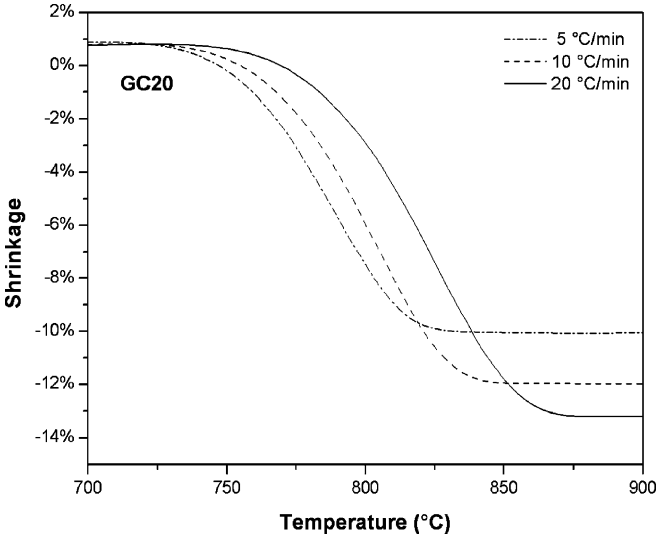

Fig. 5. Dilatometric shrinkage of GC20 during sintering at 5, 10 and 20 °C/min up to 1000 °C.

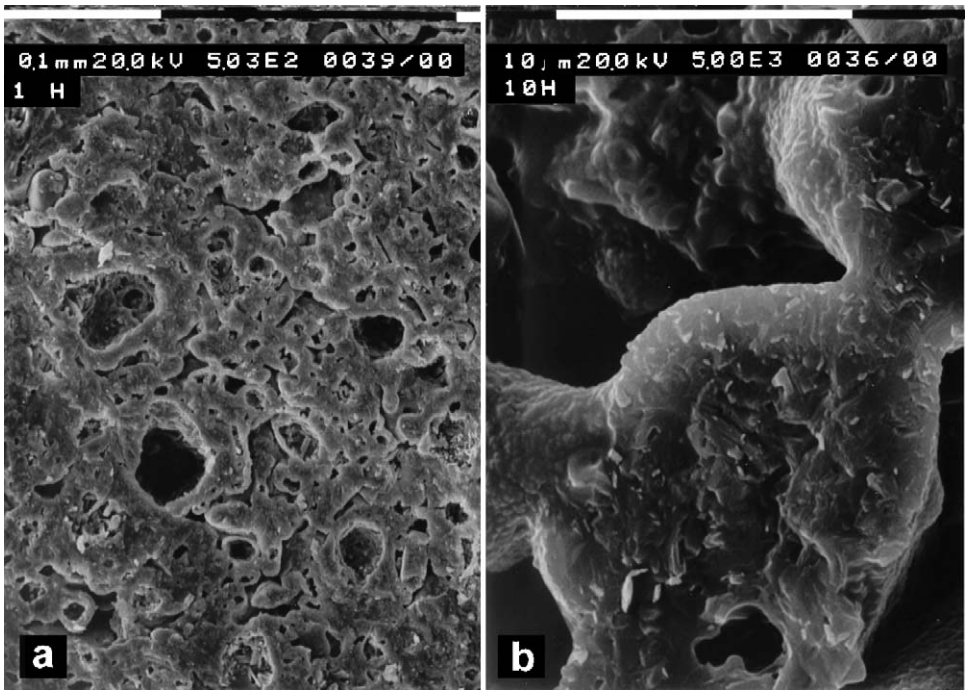

Fig. 6. SEM image of a fracture surface of GC0 sample: (a) after 1 h at 1000 °C; (b) after 10 h at 1000 °C.

samples sintered for 1 h at 1000 °C are presented in Table 2. Similar behaviour was reported for other sintered glass ceramics [16,30,31].

The morphology of GC0 and GC20, investigated by SEM observations, reveals that after 1 h heat treatment at 1000 °C, about 10–15% of residual porosity remains in the materials. Similar morphologies were obtained after 10 h with a temperature of 1000 °C.

Fig. 6a shows a fracture surface of a GC0 specimen that was heat treated at 20 °C/min up to 1000 °C for 1 h while Fig. 6b shows the same sample after 10 h of heating. In Fig. 6a, the glass particles and the residual open porosity are clearly dis-

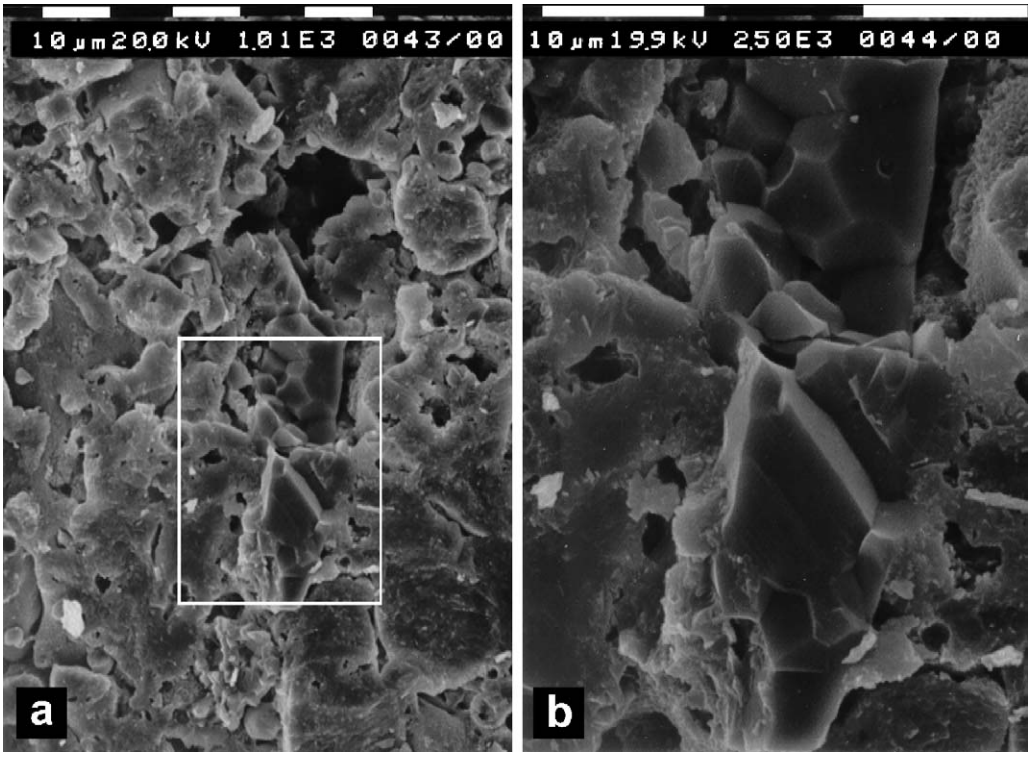

Fig. 7. SEM image of a fracture surface of GC20 sample.

Table 2
Properties of the sintered materials

Heating rate (°C/min)	ρ_{ap} (g/cm^3)	ρ_{sk} (g/cm^3)	P (%)	E (GPa)	σ_b (MPa)
GC0					
5	2.37	2.73	13 ± 2	42 ± 5	49 ± 4
20	2.41	2.70	11 ± 2	45 ± 4	59 ± 5
GC20					
5	2.38	2.86	17 ± 2	47 ± 2	53 ± 3
20	2.48	2.85	13 ± 2	59 ± 4	71 ± 4

tinguishable while Fig. 6b shows the typical necks between the particles.

Fig. 7a shows the GC20 structure after 1 h holding at 1000 °C while Fig. 7b shows the alumina particles in the glass ceramic matrix. The Al_2O_3 particles were identified by SEM-EDS analysis.

The mechanical properties are reported in Table 2 and show a positive effect due to the addition of 20% AW. At 5 K/min the bending strength and Young's modulus increase by 8% and 12% while at 20 K/min increase by 20% and 31% compared to GC0, respectively.

This behaviour can be attributed to the compressive stresses caused by the difference in the thermal expansion coefficient between the glass–glass ceramic matrix and the alumina on cooling down from the processing temperature [32,33].

4. Conclusions

The results of this study illustrate that the sintering process of vitrified MSW bottom ashes and alumina waste is inhibited by the crystallisation of pyroxene, anorthite and gehlenite, and that a residual porosity remained in the material even after prolonged thermal treatment at high temperature. For the GC20 composition at 5 °C/min, the residual porosity value is about 17% whereas, by increasing the heating rate to 20 °C/min, a porosity of 13% was obtained due to retardation in the beginning of the crystallisation process.

The addition of 20% alumina waste, AW, does not influence the crystallisation process but improves the mechanical properties. Compared to the glass ceramic sintered without additives, the bending strength and the Young's modulus increased by 20% and 30%, respectively.

References

[1] APAT-ONR, Rapporto Rifiuti 2004. http://www.sinanet.apat.it/aree/Rifiuti/.
[2] H. Van der Sloot, S. Sawell, A. Chandler, O. Hjelmer, T. Eighmiy, D. Kosson, J. Hartlen, J. Vehlow, Municipal Solid Waste Incineration Residues, Elsevier, Amsterdam, 1997.
[3] L.A. Chick, R.O. Lokken, L.E. Thomas, Basalt glass ceramics for the immobilization of transuranic nuclear waste, Ceram. Bull. 62 (4) (1983) 505–510.
[4] W. Donald, B.L. Metcalfe, R.N. Taylor, Review—the immobilization of high level radioactive wastes using ceramics and glasses, J. Mater. Sci. 32 (1997) 5851–5887.
[5] M.K. Andrews, N.E. Bibler, Radioactive demonstration of DWPF product control strategy, in: G.B. Mellinger (Ed.), Ceramic Transactions, vol. 39, Environmental and Waste Management Issues in the Ceramic Industry, The Am. Ceram. Soc. (1994) 205–211.
[6] M. Pelino, Recycling of zinc-hydrometallurgy wastes in glass and glass-ceramics materials, Waste Manage. 20 (2000) 561–568.
[7] J. Aota, L. Morin, S. Mikhail, T. Chen, D. Liang, Immobilization of hazardous elements in EAF dust by vitrification process, Waste Process. Recycl. (1995) 335–349.
[8] P. Kavouras, G. Kaimakamis, Th.A. Ioannidis, Th. Kehagias, Ph. Komninou, S. Kokkou, E. Pavlidou, I. Antonopoulos, M. Sofoniou, A. Zouboulis, C.P. Hadjiantoniou, G. Nouet, A. Prakouras, Th. Karakostas, Vitrification of lead-rich solid ashes from incineration of hazardous industrial wastes, Waste Manage. 23 (2003) 361–371.
[9] M. Erol, A. Genç, M.L. Öveçoglu, E. Yücelen, S. Küçükbayrak, Y. Taptık, Characerization of a glass-ceramic produced from thermal power plant fly ashes, J. Eur. Ceram. Soc. 20 (2000) 2209–2214.
[10] N. Menzler, H. Mortel, R. Weibmann, V. Balec, Examination of two glass compositions for the vitrification of toxic products from waste incineration, Glass Technol. 40 (1999) 65–70.
[11] M. Romero, R. Rawlings, J.Ma. Rincon, Crystal nucleation and growth in glasses from inorganic wastes from urban incineration, J. Non-Crystalline Solids 271 (2000) 106–118.
[12] M. Ferraris, M. Salvo, F. Smeacetto, L. Augier, L. Barbieri, A. Corradi, I. Lancellotti, Glass matrix composites from solid waste materials, J. Eur. Ceram. Soc. 21 (2001) 453–460.
[13] L. Barbieri, A. Corradi, I. Lancellotti, Bulk and sintering glass-ceramics by recycling municipal solid bottom ash, J. Eur. Ceram. Soc. 20 (2000) 1637–1643.
[14] A. Boccacini, G. Schawohl, H. Kern, B. Schunck, J. Ma Rincon, M. Romero, Sintered glass-ceramics from municipal incinerator fly ash, Glass-Technology 41 (2000) 99–105.
[15] T.W. Cheng, T.H. Ueng, Y.S. Chen, J.P. Chiu, Production of glass-ceramic from incinerator fly ash, Ceram. Int. 28 (2002) 779–783.
[16] A. Karamanov, M. Pelino, M. Ferraris, I. Metecovitz, Sintered glass-ceramics from MSW-incinerator fly ashes. Part II. The influence of the particle size and heat-treatment on the properties, J. Eur. Ceram. Soc. 23 (2003) 1609–16015.
[17] M. Aloisi, A. Karamanov, M. Pelino, The sintering behaviour of MSWI ash glass, J. Non-Crystalline Solids 345–346 (2004) 192–196.
[18] A. Karamanov, M. Aloisi, M. Pelino, Sintering behaviour of a glass obtained from MSWI ash, J. Eur. Ceram. Soc. 25 (2005) 1531–1540.
[19] Z. Strnad, Glass-Ceramic Materials, Elsevier, Amsterdam, 1986.
[20] W. Höland, G. Beall, Glass-Ceramics Technology, The American Ceramics Society, Westerville, 2002.
[21] B. Ryu, I. Yasui, Sintering and crystallisation behavior of a glass powder and blocks with a composition of anorthite and the microstructure dependence of its thermal expansion, J. Mater. Sci. 29 (1994) 3323–3328.
[22] R. Müller, On the kinetics of sintering and crystallization of glass powders, Glastech. Ber. Glass. Sci. Technol. 67C (1994) 93–99.
[23] Y.-M. Sung, The effect of additives on the crystallisation and sintering of $2MgO–2Al_2O_3–5SiO_2$ glass-ceramics, J. Mater. Sci. 31 (1996) 5421–5427.
[24] P.A. Trusty, A.R. Boccaccini, Alternative uses of waste glasses: issues on the fabrication of metal fibre reinforced glass matrix composites, Appl. Compos. Mater. 5 (1998) 207–222.
[25] J. Sestak, Thermophysical Properties of Solids—Their Measurements and Theoretical Thermal Analysis, Academia Prague, Prague, 1984.
[26] I. Avramov 1, E.D. Zanotto, M.O. Prado, Glass-forming ability versus stability of silicate glasses. II. Theoretical demonstration, J. Non-Crystalline Solids 320 (2003) 9–20.
[27] G.W. Scherer, Sintering with rigid inclusions, J. Am. Ceram. Soc. 70 (10) (1987) 719–725.
[28] M.N. Rahaman, L.C. Jonghe, Effect of rigid inclusions on the sintering of glass powder compacts, J. Am. Ceram. Soc. 70 (12) (1987) C348–C351.

[29] E. Zanotto, M. Prado, Isothermal sintering with concurrent crystallisation of monodispersed and polydispersed glass particles. Part 1, Phys. Chem. Glasses 42 (3) (2001) 191–198.
[30] A. Boccaccini, W. Stumpfe, D.M.R. Taplin, C.B. Ponton, Densification and crystallization of glass powder compacts during constant heating rate sintering, Mater. Sci. Eng. A 219 (1996) 26–31.
[31] P. Panda, R. Ray, Sintering and crystallization of glass at constant heating rate, J. Am. Ceram. Soc. 72 (8) (1989) 1564–1566.
[32] A. Boccaccini, P.A. Trusty, Toughening and strengthening of glass by Al_2O_3 platelets, J. Mater. Sci. Lett. 15 (1996) 60–63.
[33] F.L. Matthews, R.D. Rawlings, Composite Materials: Engineering and Science, Chapman & Hall, London, 1993.